

OPTIMIZATION OF THE DEFLAGRATION-TO-DETONATION TRANSITION

A. A. Vasil'ev

UDC 534.222.2+536.46+661.215.1

An analysis has been made of the methods of the optimizing the deflagration-to-detonation transition in fuel mixtures. Engineering formulas for designing accelerators of this process have been proposed. Certain experimental results on its optimization in plane and diverging waves, which were obtained with highly efficient accelerators, have been presented.

Keywords: combustion, detonation, deflagration-to-detonation transition, optimization.

Introduction. The use of detonation (as of the fastest regime of burning of a mixture) in different technological processes brings about problems of its practical implementation, since direct initiation of a detonation wave in fuel-air mixtures is ensured, as a rule, only by explosive charges. The ignition of the mixture by a low-power initiator followed by artificial acceleration of the flame using highly efficient accelerators up to the deflagration-to-detonation transition (DDT) is a natural alternative to explosive charges.

According to today's classification, the reaction in a fuel mixture is excited by three basic methods:

- (1) weak initiation (ignition), when only laminar combustion with velocities of propagation of the front at a level of a few centimeters a second is excited;
- (2) strong (direct) initiation, when a self-sustaining detonation wave is formed in the immediate vicinity of the initiator and then propagates in the mixture with a velocity of a few kilometers a second;
- (3) the intermediate case where the mixture is only ignited in the initial step, and then the flame front is accelerated, for natural or artificial reasons, to velocities of the "visible" flame (velocity of the flame transferred by the flow) at a level of hundreds of kilometers a second. Under certain conditions, DDT can even be subsequently implemented.

For the last case, Fig. 1 gives a typical schlieren-photosweep of the process, which shows the trajectories of transonic compression waves (generated by the initiator and the divergent flame front), the trajectory of the smoldering front, and the appearance of a few sites of spontaneous occurrence of the reaction which give rise to DDT and to a steadily propagating detonation wave.

In the issue of acceleration of the flame, of importance is the type of symmetry:

- (a) diverging waves (cylindrical, $\nu = 2$, or spherical, $\nu = 3$);
- (b) quasiplane waves (propagation in a rectilinear tube, $\nu = 1$).

In diverging laminar-combustion waves with no artificial action on the wave, the basic mechanism of acceleration is self-turbulization of the initially smooth flame front. The issue of whether an independent DDT is possible in diverging waves has been controversial so far and has been not clearly confirmed experimentally. Processes of interaction with lateral walls along with self-turbulization of the flame are of great importance in tubes and the possibility, in principle, of DDT is well known, especially for active fuel-oxygen mixtures.

Despite the established fact of DDT, data on the distance from the point of initiation to the site of occurrence of DDT in the tube L_* ("length" of the DDT, "distance" of the DDT) are quite contradictory. Such a scatter is caused by many factors, e.g., by different activities of the mixtures, the initial pressures or temperatures, the scale and degree of turbulence, the roughness of the walls, etc. Moreover, in a large-diameter tube, when the mixture is "weakly" excited by a point igniter the flame is spherical in the initial stage up to collision with the tube walls and transformation of the spherical flame into a quasiplane one requires a certain distance. For example, at a distance L from the initiation point (along the tube axis), the dimensionless nonplaneness (convexity) of the wave front can be determined as

M. A. Lavrent'ev Institute of Hydrodynamics, Siberian Branch of the Russian Academy of Sciences, Akad. Lavrent'ev Ave., Novosibirsk, 630090, Russia; email: gasdet@hydro.nsc.ru. Translated from *Inzhenerno-Fizicheskii Zhurnal*, Vol. 83, No. 3, pp. 528–538, May–June, 2010. Original article submitted August 3, 2009.

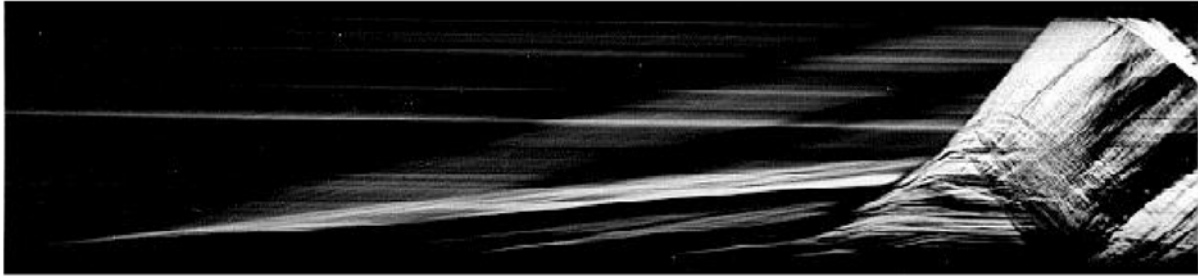


Fig. 1. Typical schlieren sweep of DDT.

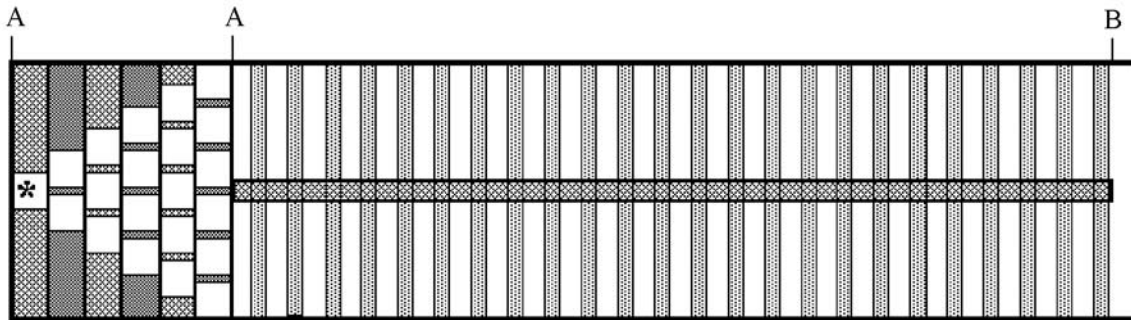


Fig. 2. Block diagram of the accelerator: region AA, generator of a quasiplane wave, region AB, multisectional DDT accelerator, *, point of ignition of the mixture.

$\delta = L(1 - \cos \varphi)/d_0$. If δ is limited by a certain natural value (e.g., $\delta = 1\%$), we obtain $L/d_0 \geq (1 + 4\delta^2)/8\delta > 12d_0$. Clearly, for large-diameter tubes, this distance L should be minimized using an additional generator of quasiplane waves, and the DDT accelerator must be placed behind the generator of quasiplane waves (Fig. 2).

Figure 3 gives certain frequently used passive elements which are characterized by individual sets of geometric parameters for acceleration of plane and divergent flames.

To accelerate the flame in rectilinear tubes we use: 1) helixes — Fig. 3a (each helix is characterized by three parameters with the dimensions of length: d_0 , d_1 , and l_1); 2) structures of singly standing rods — Fig. 3b (in addition to the dimensions of an individual rod d_2 and h_2 , the rod-type accelerator is characterized by the number of the used rods and a law of their distribution in the tube, e.g., by the step along the axis, azimuthal displacement in neighboring planes, etc.); 3) structures of disks with holes: coaxial holes — Fig. 3c or Fig. 3d, left (the characteristic dimensions are h_3 , l_3 , and d_3 ; the number of holes is of importance) or those with displacement — Fig. 3d, right (the dimensions are h_4 , l_4 , d_4 , d_5 , and z_4); 4) wire or rod screens — Fig. 3e (the characteristic parameters are the diameter of the wire, the permeability of the screen, and the distance between the screens).

For the spherically divergent flame we use: 1) hemispherical shells with holes — Fig. 3f (parameters d_6 and z_6 , number of hemispheres n , and their spatial arrangement R_1 , R_2 , R_3 , ...); 2) three-dimensional rod structures — Fig. 3g (parameters d_7 and s_7 , number of rods n_i (total and in the planes)); 3) obstacles from porous materials — Fig. 3h (radii R_{1*} and R_{2*} , porosity, number of porous layers, etc.).

Clearly, any DDT accelerator represents a multiparametric system.

On the Role of the Space and Time Factors in Optimization of DDT. The possibility of decreasing the critical initiation energy by several orders of magnitude (optimization of "strong" initiation) is attained for quite definite relations between the space and time characteristics of the initiator and the space-time parameters of the fuel mixture. Figure 4 qualitatively presents the influence of the time and space components of the energy introduced by the initiator on the conditions of initiation of the fuel mixture. For example, each mixture at a fixed pressure is characterized by such a time parameter t^* that if the discharge time is $t_0 \leq t^*$, the energy required for initiation is $E_t = \text{const} \approx E_{\min}$ and is taken for the critical initiation energy E_* ; at $t_0 > t^*$ ("delayed" discharge), E_t exceeds E_{\min} and grows with t_0 (curve E_t in Fig. 4). The influence of the space component manifests itself in a different manner: the behavior

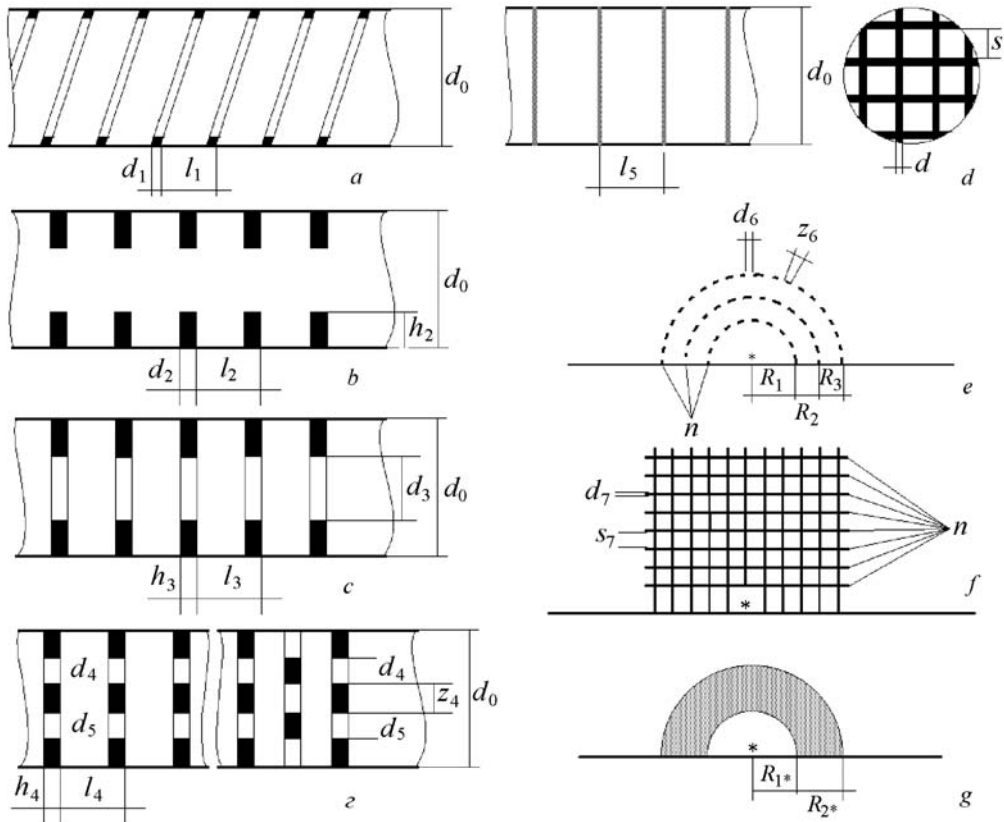


Fig. 3. Certain schemes of use of passive elements for acceleration of a "plane" and divergent flames.

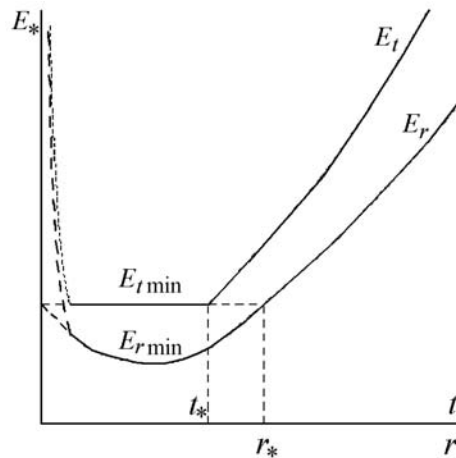


Fig. 4. Influence of the time and space components of the energy introduced from the initiator on the conditions of initiation of the fuel mixture.

of E_r is characterized by the U-shaped dependence with optimum value $E_{r\min} < E_{t\min}$. The results of investigations of the influence of only the spatial distribution of the introduced energy on the initiation of a detonation wave have shown that the minimum critical energy can be substantially reduced (by an order of magnitude or more) compared to the quantity determined with variation of only the time characteristic of the introduced energy (E_r curve in Fig. 4). For the initiation to be optimized, it is very important to elucidate all characteristic space-time parameters of the initiator in the mixture. This is all the more instructive for elucidation of the issue of the critical energy for ultrashort durations of the initiating pulse (dashed curve near the vertical axis in Fig. 4), when the power of energy introduction (supply)

tends to infinity. Sharp focusing of the region of energy supply (dashed line near the vertical axis in Fig. 4) brings about an analogous issue. The issues of optimization of initiation and the basic obtained results have been presented in [1].

Initiation is optimized with many techniques, e.g.:

- (a) spatial initiation including multiply charged circuits with variation of the number of charges and their spatial arrangement (relative position);
- (b) initiation by a pulse train with variation of the amplitude and duration of an individual pulse and of the pulse period-to-pulse duration ratio;
- (c) initiation on reflection of a shock wave from the focusing surface, including the cases where multifocal systems are used;
- (d) initiation by the jets of hot and active matters, including ionized ones;
- (e) use of promoters;
- (f) use of mixtures with distributed parameters (gradients of density, temperature, composition, etc.);
- (g) nonclassical initiation regimes.

The same techniques can also be used in optimizing DDT (in terms of the maximum decrease in the DDT distance).

Engineering Formulas for Designing DDT Accelerators. Turbulence plays the leading role in intensification of combustion (by increasing the flame surface). We know of two basic methods of turbulization of the flame: natural turbulization (self-turbulization) and the artificial one.

Self-turbulization is associated with the development of the flame front's instability (one problem of today's theory of dynamic systems).

The degree of turbulence can be increased artificially using a certain number of recurrent obstacles arranged along the direction of propagation of the wave. The prime objective of a DDT accelerator is to increase the flame front from the laminar velocity (centimeters a second) to the detonation velocity (kilometers a second) on the final length of the detonation tube. Such a great range of variation in the rate of the process (up to five orders of magnitude) is limited by the use of elements of one type (e.g., only helices, disks, or rods) in the accelerator for maximum decrease in the DDT length. The accelerator should be constructed and developed as an integrated multisectional device consisting of different elements. It is necessary that the accelerator elements turbulizing the flame be uniformly distributed over the cross section of the detonation tube and repeat its action multiple times on the combustion front with its tubewise acceleration. Obstacles of the same type on neighboring cross sections (e.g., rods) must be rotated relative to each other (azimuthal rotation about the axis), which produces additional flow turbulization. The procedure of rotation can particularly be recommended for excitation of near-spin regimes. The lengths of the sections and the dimensions of the accelerator elements and their relative position should be selected from the condition of their maximum contribution to the efficiency of the entire accelerator. It is only for the optimum relations of the geometric parameters of the DDT accelerator to the space parameters of the fuel mixture that the action on DDT will be highly efficient; for an arbitrary relation, it is slight. Unfortunately, there are no procedures for engineering design of DDT accelerators in the literature, and experimenters intuitively select one accelerator structure or another.

The idea of the accelerator elements (turbulizing the mixture) being uniformly distributed over the cross section of the detonation tube and repeating their action multiple times on the combustion front with its acceleration along the detonation tube has been used by the author in developing the engineering procedure of designing DDT accelerators. Since turbulence is one basic mechanism of acceleration of the flame, it is natural to use the theory of turbulent jets (e.g., [2]). From this theory, it is known that in the case of gas flow past a body, a turbulent layer with expanding boundaries — the external boundary, from the flow axis, and the internal boundary, toward the axis — is formed behind the body. The internal boundaries join on the axis of the body at a certain distance from it; the point of convergence is determined by the size of the body and by the angle of expansion of the internal boundary. If in a given cross section, there are a few bodies ("grid"), the external boundaries of the turbulent layers from neighboring bodies will join in addition to the joining of the internal boundaries on the axis of each body: the point of convergence of the external boundaries is determined by the distance between the bodies and the angle of expansion of the external boundary. The optimization condition is the equidistance of the points of convergence of the internal and external boundaries of the turbulent layer from the "grid" plane. This condition makes it possible to establish an opti-

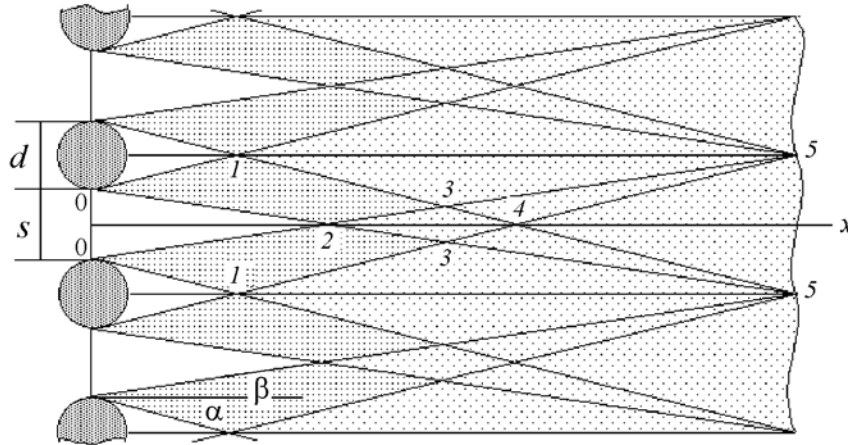


Fig. 5. Simplest scheme of turbulent zones behind obstacles: 1–5) points of intersection of the boundaries of boundary layers.

imum relation between the geometric characteristics of bodies (as turbulizing accelerator elements) in the given cross section; and to determine the coordinates of the following "grid" with turbulizing elements. Such relations represent the engineering procedure for target-oriented design of turbulizers-DDT accelerators.

The external and internal boundaries of the turbulent layer behind an obstacle begin with the points of diametral cross section; moreover, these boundaries can be approximated by linear functions (Fig. 5 gives the simplest scheme of turbulent zones behind a few obstacles located in a certain cross section of the flow). The internal boundaries from the diametral points 0 of any obstacle intersect at points 1 on the flow axis behind the obstacle:

$$x_1 = d / (2 \tan \beta) .$$

Beginning with x_1 , the turbulent layers from diametral points merge, and flow in the wake becomes turbulent (zone of weak turbulence).

If two adjacent obstacles are shifted to a certain distance s , the external boundaries of the boundary layers from these obstacles will intersect at points 2:

$$x_2 = s / (2 \tan \alpha) .$$

The region from the obstacles to the cross section x_2 is the zone of initial turbulence. Below x_2 , the flow becomes turbulent over the entire cross section. Successive interference of disturbances of the internal and external boundaries of the boundary layers from the neighboring obstacles is observed at points x_3 and x_4 . Formation of the flow with isotropic turbulence behind the obstacles occurs up to points 5:

$$x_5 = (d + 2s) / (2 \tan \alpha) ,$$

after which the turbulence only decays (basic zone with a self-similar law of decay of turbulence). Therefore, localization of the subsequent obstacle for further increase in the turbulence intensity in the region from x_2 to x_5 (this zone is called transition-type) may be assumed to be optimum.

The optimization condition is formed as the equality of the distances x_1 and x_2 . As a result the relations

$$d/s = \tan \beta / \tan \alpha \approx 1.5 , \quad x_5 \approx 10d$$

must hold, which establish the basic geometric dimensions of the turbulizing elements and their relative position and are the engineering formulas for designing DDT accelerators.

If the obstacles in a certain cross section form a structure similar to a wire screen, the permeability coefficient for the optimum condition will be equal to

$$\mu = s^2 / (s + d)^2 \approx 0.16 .$$

We should note that in wind tunnels, wire screens with $\mu \approx 0.4$ are traditionally used to form a flow with a low turbulence level (flow laminarization). When $\mu < 0.4$ the flow between the obstacles is accelerated as the jet and becomes a high-intensity turbulent flow. This is inadmissible in aerodynamics but is useful for DDT processes.

Creation of an efficient multisectional DDT accelerator makes it possible to bring experimental investigations on classifying fuel mixtures by their tendency to detonation transformation to a new level [3]. An absolute advantage of the accelerator is that classification of a specific mixture needs only one experiment in which one must record, by the trace method, the size of the cell of a multifrontal detonation wave formed using such an accelerator. The cell size a_i (or the critical energies calculated from it (E_{*i})) is basic for determination of the explosion hazard of combustibles.

Another advantage of a highly-efficient DDT accelerator is that it makes it possible to transfer investigations of fuel-air mixtures from testing-ground (with explosives) conditions to laboratory ones. Such a multisectional accelerator has been developed and optimized in the run of check experiments.

Basic Experimental Schemes. The action of a DDT accelerator on quasiplane flames has been investigated in tubes of a constant cross section and with a diameter $d_0 = 20\text{--}250$ mm for acetylene, hydrogen, ethylene, propane, methane, acetone vapor, gasoline, hydrogen peroxide, dimethyl hydrazine, ammonia, and others mixed with hydrogen and air. In the multisectional accelerator, we changed the types of turbulizing elements, the degree of blocking of the tube cross section, and the law of spatial arrangement of the elements both over the cross section and along the tube.

The velocity of the formed detonation wave after the multisectional accelerator was measured by ionization gauges installed along the tube at equal intervals. Signals from the gauges were fed, via amplifiers, to frequency meters operating in the regime of measurement of time intervals. The wave was assumed to be stable if the readings of five gauges in use gave the velocity of detonation with a scatter no higher than 2% on all kinds of gauge lengths. Detonation tubes of diameter 100 and 250 mm were used for fuel-air mixtures. The cells were measured by the traditional trace procedure on smoked metallic foils tightly fitting to the interior tube surface (dimensions of the foil: length 200 mm and width πd_0).

Highly efficient multisectional DDT accelerators were implemented for each individual tube of different diameter (on the basis of the proposed ideas and relations).

Divergent flames were investigated in a cylindrical explosion chamber (diameter and length ≈ 200 mm) with transparent windows along the lateral surface. "Point" excitation of the mixture in the first run of experiments was effected by a "weak" electric discharge of a spark plug via an electrode (diameter 1 mm) at the end of the explosion chamber on its axis. The abandonment of the thermal igniter (without a shock wave) was due to the uncontrolled scatter of the moment of ignition of the mixture with respect to the moment of feed of a thermal pulse; its replacement by the "weak" electric discharge was dictated by the necessity of synchronizing with the recording equipment (ultra-high-speed photochromatograph optically mated with an IAB-458 shadow device). The "weakness" of the initiator manifested itself in the fact that we observed only the process of low-rate burning of the mixture without any DDT manifestations in the working range of pressures. The detonation wave in the mixture in question was excited only at pressures nearly thrice as high as the working pressure, i.e., the discharge energy was nearly an order of magnitude lower than E_* . For this excitation energy, the initial stage of acceleration of the laminar-to-turbulent flame to form a shock wave was fairly short. The electric discharge from the outset produced a shock wave whose velocity exceeded the velocity of sound only slightly; it was noticeably smaller than the value for which we observe a classical DDT where a high-power nucleation site for an explosion-type chemical reaction, whose action ensures the subsequent DDT, occurs in the region between the shock wave and the flame front.

The electric discharge ensured only point ignition. In the second run of experiments, DDT was optimized by the scheme of multipoint (multisite) ignition of the mixture. In the multipoint scheme, it was necessary to increase the number of the electrodes and to achieve their synchronism of action. Change in the configuration of the spatial arrangement of the electrodes brought about additional technological problems. To eliminate the problems of multielectrode ignition, we carried out most of the experiments according to the following scheme: the electrode of "weak" discharge was arranged at the vertex of the cone cavity (prechamber) diverging toward the explosion chamber (cone angle 10° , outlet-hole diameter 40 mm); the multisite scheme of excitation of the flame in the volume was implemented using thin disks with holes of different shapes and spatial arrangements relative to each other, which were in-

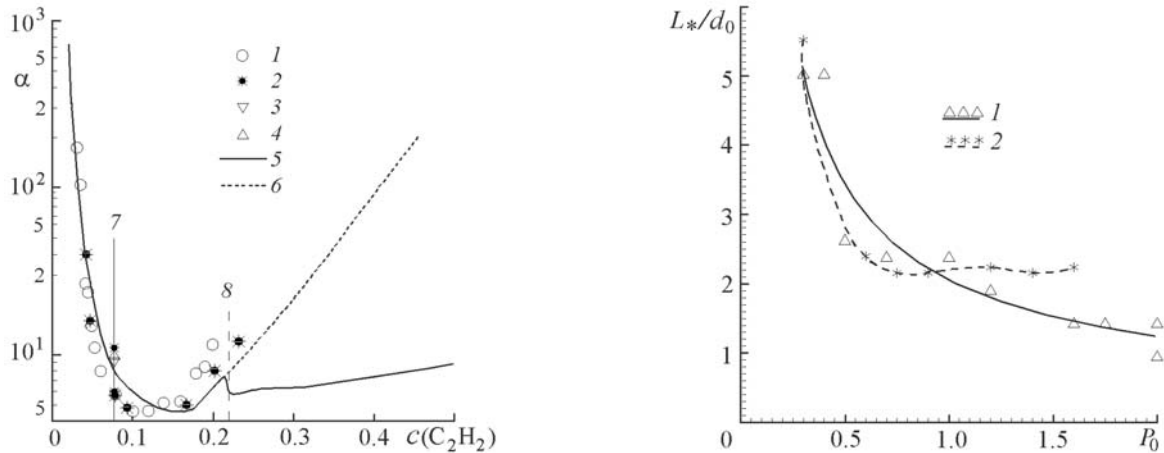


Fig. 6. Size of the detonation cell a vs. mole concentration of the fuel c (C_2H_2) in acetylene-air mixtures ($P_0 = 1$ atm): 1–4) experimental data from [8, 1, 9, 10] respectively; verticals 7 and 8) stoichiometric and equimolar mixtures; bifurcation of the calculated curves to the right of 8 is due to allowance for carbon condensation in detonation products (curve 5) compared to the calculation where carbon is considered only in the gaseous phase (curve 6). a , mm.

Fig. 7. Distance of DDT formation L^* in the tube of $d_0 = 250$ mm from the initial pressure P_0 for hydrogen-air (1) and acetylene-air (2) stoichiometric mixtures. P_0 , atm.

stalled in the plane of the cone's outlet hole. The flame passing through such holes ensured a spatial distribution of the nucleation sites of ignition in the explosion chamber and the synchronism of their action. Without a disk, the scheme modeled a quasisplane homogeneous igniter with a dimension equal to the diameter of the cone's outlet hole. The working range of initial pressures of the mixture P_0 was from the pressure at which low-rate burning was recorded throughout the length of the explosion chamber up to the pressure at which a spherical detonation at which was excited just behind the disk.

We should point to three aspects associated with the generation of turbulence in the multisite scheme: 1) the occurrence of large-scale turbulence due to the motion of the gas through the holes in the disk; 2) the action (as early as the stage of propagation of the flame in the cone) of compression waves reflected from the disk on the combustion front additionally to the flame self-turbulization, which gives rise to small-scale turbulence; 3) the spatial interaction of the compression waves with each other and with the flame front directly in the explosion chamber now. The contribution and influence of each source of turbulence of its development are dependent on the initial pressure of the mixture.

The spatial redistribution of the nucleation sites for ignition was investigated on the simplest schemes:

- (a) the multisite scheme (igniters of radius r uniformly arranged over the area of the cone's outlet hole of diameter d ; the number of the igniters was n , $4\pi r^2 < d^2$);
- (b) igniters of radius r were uniformly arranged in a circle of radius $R > d/2$ (as n increased, this discrete igniter transformed into an annular one);
- (c) the linear scheme (a single rectilinear igniter and a few sources arranged in parallel or at an angle to each other).

The structure of the explosion chamber made it possible to additionally place plane metal screens at a certain distance from the cone's outlet hole and to investigate their influence on the DDT (we varied the size of the screen squares and the number of the screens and their spatial orientation relative to each other and to the cone's outlet hole).

Results of DDT in Quasisplane Waves (of the Tube). Once the structure of the multisectional accelerator had been optimized, we checked the possibility of forming a self-sustained detonation wave on the scale of a laboratory setup in weak initiation for a stoichiometric mixture of methane with air (one of the most difficult to excite mixtures: in this mixture, in the tube of $d_0 = 100$ mm without a DDT accelerator, we observed only combustion with a rate of

the order of 1 m/sec; with an accelerator, we observed the formation of a spin detonation wave on the length $L_* \approx 2500\text{--}3000 \text{ mm} \approx (25\text{--}30)d_0 \approx 10a!$

Successful solution of the problem of DDT acceleration on the scale of laboratory equipment has also been confirmed on other fuel-air mixtures and fuel-oxygen mixtures. For example, to classify the explosion hazard of acetylene we performed experimental investigations in the tube of $d_0 = 100 \text{ mm}$ on explosive $\text{C}_2\text{H}_2 + 2.5(\text{O}_2 + z\text{N}_2)$ and C_2H_2 -air mixtures. In the first run, we varied the initial pressure P_0 in the range (0.04–1.40) atm and the amount of the added nitrogen $z = 0\text{--}3.76$; in the second run, we varied the stoichiometric coefficient ϕ at constant pressure $P_0 = 1.0 \text{ atm}$. The bounds of ϕ were the lower and upper (c_{low} and c_{up}) concentration limits of the fuel mixture.

As the experiments have shown, the DDT accelerator successfully forms the detonation wave in a fairly wide range of concentrations. Figure 6 gives as an example data on the size of the cell in the detonation wave formed using this DDT accelerator (for acetylene-air mixtures). The detonation wave is excited when the composition "departs" from that stoichiometric ($\phi = 1.0$) and approaches a composition corresponding to the lower detonation limit ($\phi = \phi_{\text{low}}$); for $\phi < \phi_{\text{low}}$, we only record high-rate-combustion regimes. With "departure" from $\phi = 1.0$ in the opposite direction (enrichment of the mixture) the size of the cell decreases to a certain minimum in the region $\phi \approx 1.5$, and then $a(\phi)$ grows. Beginning with $\phi \approx 2$, the amount of soot in detonation products noticeably increases: for $\phi \approx 2.5$, a layer of thickness $\approx 2\text{--}3 \text{ mm}$ is formed on the tube walls, which makes it very difficult to process trace marks.

At $P_0 = 1.0$, the system "generator of quasiplane waves + multisectional accelerator" guarantees DDT and the formation of a multifrontal detonation wave in a tube of diameter 250 mm in acetylene-air and hydrogen-air stoichiometric mixtures at record-short distances of 450 mm (about 2 calibers)! The results of these experiments are presented in Fig. 7; the quantity L_* is reckoned from the beginning of the multisectional accelerator and is made dimensionless by means of the tube diameter. The experimental values of $a(P_0)$, $a(z)$, $a(\phi)$, etc. obtained using the multisectional accelerator have a typical U shape.

Results of DDT in Diverging Waves (Spherical Case). In the scheme with a spatial initiator distribution, in addition to the critical energy, we can use, for the sake of comparison, the critical diameter of diffraction of the detonation wave d_{**} . Diffraction of the detonation wave is a method of initiating a spherical detonation wave in the mixture volume using the detonation wave performed in the rectilinear tube of diameter d_0 . Initiation of the mixture in the volume is observed on the condition that the tube diameter exceeds the value d_{**} which is critical for these conditions; if d_0 is less than d_{**} , we observe the decay of the initiating wave and the burning of the mixture in a turbulent-combustion regime. The critical diffraction diameter acts as an unusual equivalent of the critical initiation energy.

In this scheme, the check of the "weakness" of the electric discharge in initiating the mixture in the vertex of the cone has shown that in the working pressure range, we only observe turbulent-combustion regimes, i.e., the initiator energy is known to be lower than the critical energy of initiation of the spherical detonation wave. Deflagration-to-detonation transition occurs at much higher pressures.

Figure 8 gives experimental data on the coordinate X_* of DDT in the spherical wave as a function of the initial pressure of the $\text{C}_2\text{H}_2 + 2.5\text{O}_2$ mixture. The dashed vertical line P_0^* (right) corresponds to the formation of the detonation wave near the outlet hole of the cone at exit of the flame from the cone to the volume (when the cone's outlet hole is open). At $P_0 > P_0^*$, we observe direct excitation of spherical detonation — region I — in the volume. The dashed vertical line $P = P_0^{**}$ (left) corresponds to the diffraction initiation of the mixture on the condition that the tube diameter is equal to the diameter of the cone's outlet hole. Regimes of high-rate turbulent DDT-free combustion are recorded in the explosion chamber in the range $P_0^{**} < P < P_0^*$.

The experiments have shown, e.g., on the $\text{C}_2\text{H}_2 + 2.5\text{O}_2$ mixture, that

$$P_0^* \approx 8P_0^{**}.$$

Initiation of spherical detonation on diffraction of the detonation wave for this mixture is characterized by the relation

$$d_{**}/a \approx 8 \pm 2,$$

then the excitation of the spherical detonation wave on flame diffraction and subsequent DDT increases this value to

$$d_{\text{f}}/a \approx 64 \pm 16,$$

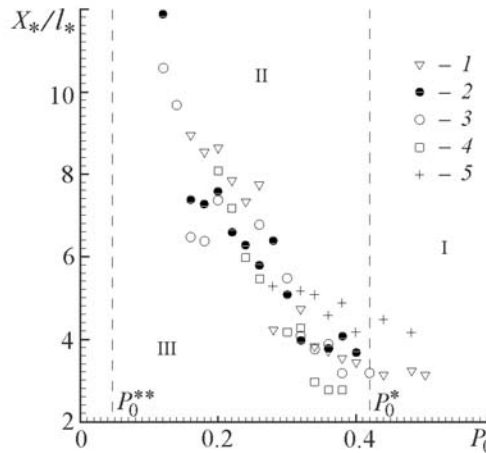


Fig. 8. Distance of DDT formation in a diverging wave X^* using multisite schemes of the DDT accelerator vs. initial pressure P_0 : 1) three linear igniters connected in the circuit of a regular triangle; 2) 19 igniters of diameter 5 mm each uniformly arranged within a circle of diameter 40 mm; 3) six igniters of diameter 5 mm arranged in a cycle of diameter 35 mm; 4) two linear parallel igniters shifted relative each other; 5) two linear parallel igniters without a shift (contacting). P_0 , atm.

since $a \sim 1/P_0$.

If we pass on to the multisite scheme of excitation of the flame in the explosive-mixture volume (using thin perforated disks in the outlet cross section of the cone), the experimental points in the region of high-rate turbulent combustion $P_0^{**} < P < P_0^*$ subdivide this region into subregion III with spherical combustion (deflagration) and subregion II where the formation of spherical detonation due to DDT is observed. The appearance of subregion II unambiguously testifies that the spatial redistribution of the ignition sources contributes to the DDT. In Fig. 8, the quantity X_* is reckoned from the plane of the outlet disk and is made dimensionless by means of the characteristic dimension of an individual igniter l_* ; points 1–5 denote the experimental data corresponding to different schemes of spatial arrangement (layout) of nucleation sites for ignition.

1. The multipoint scheme consisting of 19 holes of diameter $2r = 5$ mm (one central hole, six holes in a circle of radius $R_1 = 10$ mm, and 12 holes, of $R_2 = 17.5$ mm) uniformly arranged on the area of the cone's outlet cross section: points 2 in Fig. 8; the diameter of an individual hole is denoted by l_* . The velocity of compression waves going out to the volume is $\approx 1.5c_0$. When the amplitudes of the compression waves are very low, the processes of shock-wave self-ignition are of little importance. Turbulization of the mixture and direct action of the combustion products on it are mainly responsible for the turbulization of the process. Although it is unlikely that the use of the cell size a will be correct to describe DDT having no pronounced structure with a characteristic spatial dimension, we note that the quantity a corresponding to the boundary pressure for this scheme (when DDT is still recorded) turns out to be nearly half as large as the diameter of an individual hole: $a \approx r$.

2. The sixpoint scheme with holes of $2r = 5$ mm arranged in a circle of radius $R = 17.5$ mm (experimental data for this layout are denoted by points 3).

3. Linear igniters were modeled using slotted disks. A 4×30 mm slot diminished the flame area by nearly an order of magnitude, just as in the six-point layout diagram, but there was no large-scale turbulence in this case. This resulted in the fact that with decrease in the pressure from P_0^* the DDT region extended only to a pressure of $\approx 0.6P_0^*$ (5). Two parallel 4×30 mm igniters with shift $W = 2h$ led to an extension of the DDT region to a pressure of $\approx 0.4P_0^*$ (4). Finally, three linear igniters connected in the circuit of a regular triangle (inscribed into the outlet hole of the cone) ensured DDT up to a pressure of $\approx 0.3P_0^*$ (1), which is nearly equivalent to the multipoint scheme with $n = 19$ (2). For these experiments, l_* in Fig. 8 denotes the slot width h .

We particularly note that the spatial distribution of the ignition sites makes it possible, under certain conditions, to decrease the DDT distance by orders of magnitude.

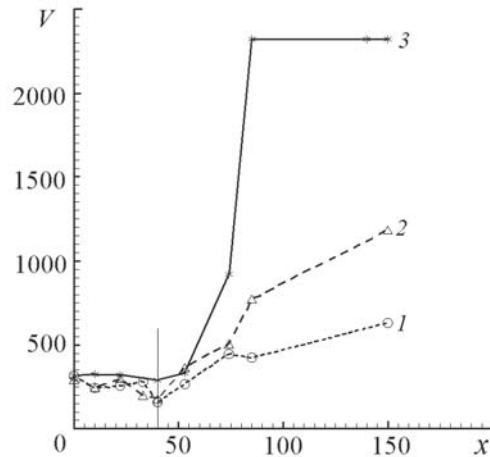


Fig. 9. Growth in the "visible" flame velocity V in a diverging wave with distance of the wave x from the diffractive cross section on interaction with the turbulizing screen at different pressures: 1) 0.10, 2) 0.18, and 3) 0.28 atm. V , m/sec; x , mm.

Figure 9 plots the "visible" velocities of the divergent flame (flame velocity plus flow velocity) versus the distance (x is reckoned from the plane of the outlet disk) in artificial flame turbulization using screens. It is seen that transonic velocities of propagation of the flame front are recorded in front of the screen; behind the screen, the velocity increases and the DDT probability grows, which is particularly noticeable, as the initial pressure of the mixture increases (passage from curve 1 to 3). Photosweeps make it possible to evaluate the compression-wave velocity and the visible flame velocity (along the axis of the explosion chamber). Subtracting the mass velocity of the gas behind the shock wave from the visible flame velocity, we obtain the rate of combustion for particles. This quantity is noticeably higher than the rate of laminar combustion under these conditions, which is characteristic of combustion in strongly turbulent flows.

The explosion hazard of fuel mixtures is evaluated by initiation energies: the lower the energy, the more hazardous the mixture. From this viewpoint, the $2\text{H}_2 + \text{O}_2$ mixture ranks much below the $\text{C}_2\text{H}_2 + 2.5\text{O}_2$ mixture. The experiments carried out with the hydrogen mixture have confirmed the basic conclusion on DDT intensification in spatial ignition of the mixture. Thus, when the "weakness" of the source with an open outlet cross section of the cone was checked, detonation could not be excited up to $P_0 = 2.5$ atm; when the multisite scheme 2 (Fig. 8) was used, DDTs were observed both at $P_0 = 2.5$ atm and with decrease in P_0 from 2.5 to approximately 0.8 atm. Analogous results were also obtained on other schemes (e.g., [4-7]).

Conclusions. We have proposed engineering formulas for designing DDT accelerators using which the DDT efficiency can be raised substantially.

Highly efficient DDT accelerators, which make it possible to transfer investigations on the explosion hazard of fuel mixtures from testing-ground conditions to laboratory ones, have been developed.

The effect of considerable (tens or even hundreds of times) decrease in the length of the DDT zone in the case of spatial distribution of the igniters has been established. This means that for the spatial distribution of the introduced energy, there are conditions under which the DDT efficiency and hence the explosion hazard of the mixture can become much higher compared to the lumped source. This effect makes one pay special attention to the classical ideas of the criteria of explosion hazard of fuel mixtures. The requirements of fire and explosive safety in the field of spatial influence of the initiator must be more stringent. For this reason, the limit of explosive safety in the activity series of explosive mixtures must be changed.

Under certain conditions, DDT can be a more serious hazard than detonation by virtue of the large spatial scale of the leading part of the nonstationary gasdynamic complex consisting of a shock wave, an induction zone, and a chemical-reaction zone.

We have obtained new experimental data on the conditions of DDT intensification for the cylindrical and spherical cases of symmetry.

This work was carried out with partial financial support from the Russian Foundation for Basic Research (grant 08-01-00347a), the Siberian Branch within the framework of Program No. 13 of the Russian Academy of Sciences "Fundamentals of Development of Energy Systems and Technologies," and the Leading Scientific School of the Russian Federation "Mechanics of Shock and Detonation Processes."

NOTATION

a , detonation-cell size, mm; c_0 , velocity of sound in the original mixture, m/sec; $c(\text{C}_2\text{H}_2)$, mole concentration of the fuel in the fuel mixture; c_{low} and c_{up} , mole concentrations of the fuel which correspond to the lower and upper limits; d , diameter of the wire for the turbulizing screen, mm; d_0 , diameter of the detonation tube, outside diameter of the helix, mm; d_1 , diameter of the wire for the helix, mm; d_2 , diameter of a single rod element, mm; d_3 , d_4 , and d_5 , diameter of the opening of the disk element, mm; d_6 , diameter of an individual hole in the accelerator's hemispherical element, mm; d_7 , diameter of the rod element in the "screen" structure, mm; d_f , critical diffraction diameter of the flame, mm; d_{**} , critical diffraction diameter of the detonation wave, mm; E_* , critical energy, J; E_r , space component of the introduced energy, J; E_t , time component of the introduced energy, J; E_{min} , minimum critical energy, J; h , width of the slot in the disk, mm; h_2 , height of the rod element, mm; h_3 and h_4 , disk thickness, mm; L , distance from the point of initiation to the detonation-wave front along the tube axis, mm; L_* , distance from the point of initiation to the DDT point, mm; l_1 , lead of the helix, mm; l_2 , distance between rod elements along the tube axis, mm; l_3 and l_4 , distance between disk elements along the tube axis, mm; l_5 , distance between turbulizing screens along the tube axis, mm; l_* , characteristic scale of the initiator (transverse dimension — width — for initiation of a cylindrical wave), mm; n , number of elements; P , pressure, atm; P_0 , initial pressure of the mixture, atm; P_0^* , pressure at which a spherical detonation wave is excited at exit of the flame and subsequent DDT, atm; P_0^{**} , pressure at which a quasispherical detonation wave is excited in the procedure of diffraction reinitiation of multifrontal detonation (exit of the quasiplane detonation wave from a constant-cross-section tube to the volume), atm; R_1 , R_2 , R_3 , ..., radii of hemispherical accelerator elements, mm; R_{1*} and R_{2*} , radii of hemispherical porous accelerator elements, mm; $s \times s$, dimension of the flow section of an individual cell of the turbulizing screen, mm; $s_7 \times s_7$, dimension of the flow section of an individual cell of the "screen" rod structure, mm; t_0 , characteristic discharge time, μsec ; t^* , characteristic time parameter of the mixture, μsec ; V , flame velocity, m/sec; W , distance between linear igniters, mm; x , distance from the screen downstream, mm (Fig. 5); x_1 , x_2 , x_3 , x_4 , and x_5 , coordinates of intersection of the boundaries of boundary layers behind the screen, mm; x , distance from the diffractive cross section, mm (Fig. 9); X_* , distance from the diffractive cross section to the point of DDT in the diverging wave, mm (Fig. 8); z , dimensionless coefficient characterizing the proportion of nitrogen and oxygen in the mixture ($z = 3.76$ for air); z_4 , size of the bridge between holes in the disk, mm; z_6 , size of the bridge between holes in the hemispherical accelerator element, mm; α , angle of deviation of the external boundary of the boundary layer to the flow axis; β , angle of deviation of the internal boundary of the boundary layer to the flow axis; δ , nonplaneness (convexity) of the wave front in the discharge; ϕ , stoichiometric coefficient equal to the ratio of the mole fraction of the fuel in a given mixture to the mole fraction of the fuel in a mixture of the stoichiometric composition; ϕ_{low} , stoichiometric coefficient corresponding to the lower concentration limit of detonation; φ , half-angle at which the wave front is seen from the point of initiation; μ , permeability coefficient of the screen; ν , symmetry index (1, 2, and 3, for the plane, cylindrical, and spherical cases).

REFERENCES

1. A. A. Vasil'ev, Modern state of initiation problem and ways of its optimization, *European Combustion Meeting*, ECM2005, Louvain-la-Neuve, Belgium, 3–6 April 2005, CD: ECM2005, *Proc. European Combustion Meeting*, Louvain-la-Neuve, Belgium (2005).
2. G. N. Abramovich, S. Yu. Krashennnikov, A. N. Sekundov, and I. P. Smirnova, *Turbulent Mixing of Gas Jets* [in Russian], Nauka, Moscow (1974).
3. A. A. Vasil'ev, Optimization of accelerators of deflagration-to- detonation transition, in: *Confined Detonations and Pulse Detonation Engines*, TORUS PRESS Ltd., Moscow (2003), pp. 41–48.

4. A. A. Vasil'ev, Initiation of gas detonation in the case of spatial distribution of sources, *Fiz. Goreniya Vzryva*, **24**, No. 2, 118–124 (1988).
5. A. A. Vasil'ev, Spatial excitation of multifrontal detonation, *Fiz. Goreniya Vzryva*, **25**, No. 1, 113–119 (1989).
6. N. V. Bannikov and A. A. Vasil'ev, Multisite ignition of a gaseous mixture and its influence on deflagration-to-detonation transition, *Fiz. Goreniya Vzryva*, **28**, No. 3, 65–69 (1992).
7. A. A. Vasil'ev, Specific features of application of detonation in propulsion systems, in: S. M. Frolov (Ed.), *Pulse Detonation Engines* [in Russian], TORUS PRESS, Moscow (206), pp. 129–158.
8. R. Knystautas, C. Guirao, J. H. Lee, and A. Sulmistras, Measurement of cell size in hydrocarbon-air mixtures and predictions of critical tube diameter, critical initiation energy and detonation limits, in: J. R. Bowen, N. Manson, A. K. Oppenheim and R. I. Soloukhin (Eds.), *Dynamics of Shock Waves, Explosions and Detonations*, Vol. 94 of *Progress in Astronautics and Aeronautics*, New York (1983), pp. 23–37.
9. D. C. Bull, J. E. Elsworth, P. J. Shuff, and E. Metcalfe, Detonation cell structures in fuel-air mixtures, *Combust. Flame*, **45**, No. 1, 7–22 (1982).
10. R. Knystautas, J. H. Lee, and C. M. Guirao, The critical tube diameter for detonation failure in hydrocarbon-air mixtures, *Combust. Flame*, **48**, 63–83 (1982).